Crowd Dynamics on a Moving Platform: Mathematical Modelling and Application to Lively Footbridges

Fiammetta Venuti*, Luca Bruno
Politecnico di Torino, Department of Structural Engineering and Geotechnics
Viale Mattioli 39, I-10125, Torino, Italy
fiammetta.venuti@polito.it
luca.bruno@polito.it

Nicola Bellomo
Politecnico di Torino, Department of Mathematics
Corso Duca degli Abruzzi 24, I-10129, Torino, Italy
nicola.bellomo@polito.it

Abstract—This paper proposes a mathematical model and a computational approach to study the complex multiphysical non linear coupled system that results from the interaction between a moving platform and the pedestrians who walk on it. The described method is based on the mathematical and numerical decomposition of the coupled system into two subsystems and on the two-way interaction between them. In particular, the dynamics of the crowd is modelled referring to a macroscopic description in analogy to that of a compressible flow. The proposed approach is applied to the lateral vibrations of footbridge decks under human-induced excitation. First, the computational parameters of the model are optimised. Then, the effects of the crowd initial density and of the runnability conditions are evaluated on a motionless platform. Finally, the results obtained from the simulations of the crowd-structure interaction are commented on.

Keywords—pedestrian dynamics; crowd-structure interaction; synchronization; footbridge; lateral vibration; computational simulation.

1 Introduction

The excessive vibrations induced by synchronous lateral excitation exerted by pedestrians who walk on crowded footbridges have attracted increasing public attention in the last few decades [1] from the earliest cases in the nineties [2] up to the well-known case of the London Millennium Bridge which was opened on 10 June 2000 [3]. The growing frequency of occurrence of these phenomena is primarily due to the increasing strength of new structural materials and longer spans of new footbridges, accompanied by the aesthetic requirements for greater slenderness. Up to date, such kind of dynamic lateral loads have never involved structural failures, but have often caused discomfort for the users and the temporary closure of the footbridges. Neverthless, this reduced serviceability represents a severe problem for its economic and social outcomes, bearing in mind that these structures often represent a "visiting card" of the town where they are built and that high crowding generally occurs during the opening day of the structure. The afore mentioned reasons have motivated the recent and intense research activity, to date mainly developed in the field of civil engineering and structural dynamics. The wide scientific literature published in recent years, and recently reviewed in [1], testifies this effort and provides a useful background to comment on the actually employed approaches and to introduce the one proposed in this work.

The problem has generally been tackled starting from an empirical approach. The studies can be roughly classified according to the addressed scales of the phenomenological observation of the system: the small scale (i.e. the behavior of the single pedestrian) and the large scale (i.e. the crowd-structure interaction and the structural response).

*Corresponding author – fax number: (+39) 011.564.4999.

The measurements of the forces exerted by one pedestrian walking on a fixed or moving platform belong to the first class of studies. Walking forces on motionless platform have been widely studied in the field of biomechanics together with that of footbridge dynamics. The components of a single step walking force in all significant directions (vertical, lateral and longitudinal) have been measured by Andriacchi et al [4]. In particular, if a perfect periodicity of the force is assumed, the lateral component shows a fundamental frequency equal to 1 Hz, i.e. half the pacing frequency of normal walking [1]. The lateral force peak amplitude is approximatively equal to 30 N. Significant correlations of many walking parameters (among others, the stride length and the walking velocity) have been pointed out for the vertical component by Wheeler [5].
Laboratory tests involving a single pedestrian walking on platforms or treadmills forced to move laterally (e.g. in [3] [6] [7]) allow important data about the relationship between the platform motion and the lateral force component to be obtained. In fact, because of the attempt to maintain the body balance on the laterally moving platform, the pedestrian adapts his step frequency to that of the platform (synchronization) and he walks with his legs more spread. Hence, the lateral motion of the upper part of the torso increases and the resulting force in turn grows. The latter is usually expressed in terms of Dynamic Load Factor (DLF) as the ratio between the force itself and the pedestrian static weight. The same tests point out that different pedestrians can show different sensitivities to platform motion, so that a factor is introduced to describe the degree of synchronization, i.e. to estimate the mean probability that individuals will synchronise their footfall rates to the swaying rate of the platform [3].

To the authors' knowledge, the large scale has been studied up to now through: i) the examinations of the measured structural oscillations; ii) the observation of the videos recorded during crowd events on actual bridges [2] and full-scale tests on monitored structures [3].
Let us first refer to the studies about the dynamic response of the structures. These studies suggested several authors (e.g. in [7], [8], [9]) to refer to an interaction phenomenon between fluid flow and structures widely studied in wind engineering and commonly known as lock-in. In this case, the cross-flow oscillations of a bluff structure are due to and interact with the shedding of vortices in its wake. Even though the vortex-induced and crowd-induced oscillations differ in their causes, they show analogous features about the structural response. In a given range of the incoming wind velocity (the so-called lock-in region), the vortex-shedding frequency is in fact constant and equal to the frequency at which the structure oscillates, rather than being a linear function of the wind velocity, as stated by the Strouhal law. In other terms, the structural motion affects the wind flow (or crowd flow) so that synchronization occurs and the resonance condition takes place. Furthermore, both phenomena are self-limited, in the sense that structural oscillations do not proceed to divergent amplitudes but enter a limit cycle even though the structural damping is null.

As far as the second class of studies is concerned, the observation of the videos permits one to qualitatively point out the great complexity of the overall mechanical system, mainly due to the two-way interaction between the crowd and the structure and to the non homogeneous crowd distribution along the deck (density, velocity). In particular, the motion of each pedestrian is affected by the presence of the surrounding people, especially by the flow of the pedestrians in front. The higher the crowd density, the more likely the possibility that pedestrians can see each other, walk shoulder-to-shoulder and subconsciously synchronize their pacing rate. Hence, a second kind of synchronization takes place apart from the one between each pedestrian and the structure. An attempt to take into account the effects of the crowd density on synchronization among pedestrians has been made by Grundmann et al. [10]: three human-induced force models, which correspond to different but spatially homogeneous pedestrian densities and that have to be separately considered, were proposed. Hence, the problem of actual non homogeneous crowd still remains open.

According to the authors, the models proposed so far, and previously briefly summarized, encountered some difficulties in taking some important aspects of the problem into account, i.e. the self-organization effects that occur in pedestrian flow. These effects could be induced due to the features of the platform (e.g. shape, slope, presence of obstacles) or to the platform vibrations. They may involve discontinuities of the crowd density and velocity along the deck up to obstructions, traffic jams or stop-and-go phenomena. From this point of view, walking people cannot be simply described by means of a given force model but need to be directly modelled as a part of the complex dynamic system.

Traffic dynamics have been widely analysed and modelled for vehicular flows in the field of applied mathematics and transportation engineering since the beginning of the seventies. Some books [11] [12] and expository papers [13] [14] provide a useful background of the field of research. Generally speaking, the models developed in literature describe the evolution in time and space of the flow conditions, i.e. car density and velocity. The first task in modelling granular traffic flows is to select the correct observation and representation scale, the choice of which determines three different classes of frameworks. A microscopic description corresponds to modelling the dynamics of each single vehicle under the action of the surrounding vehicles. Statistical or

mesoscale description, in a framework close to the one of the kinetic theory of gases, consists in the derivation of an evolution equation for the probability distribution function on the position and velocity of a vehicle along a road. Macroscopic description, which is analogous to that of fluid dynamics, refers to the derivation, on the basis of conservation equations and material models, of an evolution equation for the mass density, linear momentum and energy, regarded as macroscopic observable quantities of the flow of vehicles assumed to be continuous. All the above mentioned approaches have been extended to the simulation of crowd dynamics [15]. Macroscopic modelling has been applied since the pioneering works of Henderson [16] in the seventies. Hoogendoorn and Bovy [17] applied, among others, the mesoscale description to the pedestrian traffic. A relevant number of models have been developed in recent years in the framework of the microscopic description, such as the social force model [18] or the cellular automata model [19]. In the last decade, special attention has been devoted to the microsimulation of pedestrian crowds, since it is more flexible and may be easily applied to panic conditions and emergency evacuation.

To the best of the authors' knowledge, up to now none of the three previously mentioned frameworks has been applied to crowd-structure interaction. This paper deals with the proposal of a mathematical model of crowd-structure interaction that includes the simulation of crowd dynamics. The model aims at representing the complex multiphysical non linear dynamic system to give, on one hand, a detailed description of the crowd flow along the deck and, on the other, to obtain synthetic results that are useful for engineers and designers. The main features of the model lie in the mathematical and numerical decomposition of the coupled system into two physical subsystems and in the two-way interaction between them [20]. A first order model based on the mass conservation equation [21] is adopted to macroscopically describe the dynamics of the crowd in the framework of hydrodynamic modelling. The structural system is modelled by means of a generalized Single Degree Of Freedom (SDOF) model [22].

The paper focuses on the description of the mathematical model and its application through computational simulation. The contents of the paper are developed in four more sections: Section 2 is devoted to the description of the set of equations governing both the crowd and the structural system; Section 3 deals with the numerical approach used to solve the equations; in Section 4 some applications are presented for both fixed and oscillating platform in order to optimize the computational approach and to discuss the main outcomings. The concluding remarks and research perspectives are developed in Section 5.

2 Governing equations

2.1 Crowd system

As stated in the previous section, mathematical modelling of crowd dynamics can be developed according to three different mathematical frameworks, respectively based on microscopic, statistical and macroscopic description [13]. In particular, first order macroscopic modelling refers to the derivation of an evolution equation for the mass density, regarded as a macroscopic quantity of the flow assumed to be continuous. Such a representation implies an approximation of the physical reality, since the distances among the pedestrians can be large enough to be in contrast with the continuity assumption of the hydrodynamic model. On the other hand, a relatively simple model is preferable to study the complexity of the crowd-structure coupled system. In addition, the lack of experimental data on crowd behaviour makes it difficult to use the other two kinds of representation. Hence, a first order hydrodynamic model in the one-dimensional (1D) spatial domain is developed in the following.

Once the representation scale has been chosen, it is useful to express all the variables involved in the problem in a dimensionless form, therefore they are scaled with respect to characteristic quantities, that is:

- L is the length of the footbridge span;
- u_M is the maximum admissible density of the crowd;
- v_M is the maximum mean velocity of the crowd.

Furthermore, let us introduce a characteristic time $T_c = L/v_M$, defined as the time necessary to cover the footbridge span L walking at the maximum mean velocity v_M. Literature [23] reports that, for a pedestrian flow, $v_M = 1.5$ m/s and $u_M = 120$ Kg/m^2, corresponding to 1.6-1.8 persons/m^2.

We can now define the independent and dependent dimensionless variables (the subscript r refers to the variable dimensional value):

- $t = t_r/T_c$ is the time independent variable;

- $x = x_r/L$ is the space independent variable;
- $u = u_r/u_M$ is the crowd mass density;
- $v = v_r/v_M$ is the crowd velocity;
- $q = u \cdot v$ is the linear mean flux.

It follows that the reference framework describing the crowd dynamics is given by the 1D mass conservation equation in its Eulerian form:

$$\frac{\partial u}{\partial t} + \frac{\partial}{\partial x}(uv) = 0. \tag{1}$$

The mass conservation equation should be closed by a phenomenological relation that links the local mean velocity to the local mass density. Actually, the lack of experimental data does not allow a specific closure equation for pedestrian flow to be tuned. Hence, different qualitative closure equations, based on some analogies between the behaviour of pedestrians and vehicles, can be proposed. In particular, pedestrians are assumed to walk at the maximum velocity if the density is below a critical value $u_c = 0.17$ [1], while v monotonically decays as u increases from the maximum value $v(u = u_c) = 1$ to $v(u = 1) = 0$, as proposed in literature for vehicular traffic flow [13]. The simplest expression is the linear equation:

$$v(u) = \begin{cases} 1 & u \leq u_c \\ \frac{1-u}{1-u_c} & u > u_c \end{cases}. \tag{2}$$

More sophisticated models can be obtained by introducing a parameter that represents the runnability conditions of the motionless deck (e.g. slope of the road, conditions of the flooring surface, environmental conditions such as a panoramic point along the span). In the following, a first closure equation comes from a fitting to experimental data on vehicular traffic proposed in [24]:

$$v(u) = \begin{cases} 1 & u \leq u_c \\ \exp\left(-\alpha \frac{u-u_c}{1-u}\right), & u > u_c \end{cases} \tag{3}$$

with the parameter $\alpha \in [0; 2.5]$. A second closure equation is proposed in this work so that

$$v(u) = \begin{cases} 1 & u \leq u_c \\ 1 + \frac{\exp[-\beta(u-u_c)/(1-u_c)]}{1-\exp(-\beta)} & u > u_c \end{cases}. \tag{4}$$

The expected range of variability of the parameter β is [0; 10]. Both equations are fitted to the experimental data reported in [24]: as shown in Fig.1, relatively larger values of α and β denote strong decay of the mean velocity with local density and hence relatively less favourable runnability conditions. In the following, equation 4 is retained since it allows the linear equation 2 for $\beta = 0$ to be recovered.

Since the dynamic system that has to be dealt with is an open system, particular attention is paid to the definition of the boundary conditions (bc) on density. At the downstream (outlet) boundary, a null von Neumann bc is imposed. If a Dirichlet bc is set at the upstream (inlet) boundary, unphysical situations can arise when a backward moving flow approaches the boundary with a higher density than that assumed at the inlet. The problem is herein solved by switching from a Dirichlet to a von Neumann bc in the case of congested traffic near the upstream boundary.

2.2 Structural system

The structural system is modelled as a 1D beam of overall length L and cross-section width B. First, a modal analysis is performed in order to search, select and extract the significant eigen vector $\boldsymbol{\varphi}(x)$, whose circular frequency ω falls in the lock-in region ($[2\pi \cdot 0.8; 2\pi \cdot 1.2$ rad/sec] [25]). Hence, the selected mode is used to build a generalized SDOF model whose dynamics is described by the non-dimensional Lagrangian form of the momentum conservation equation:

$$m^* \ddot{Z}(t) + c^* \dot{Z}(t) + k^* Z(t) = F^*(t), \tag{5}$$

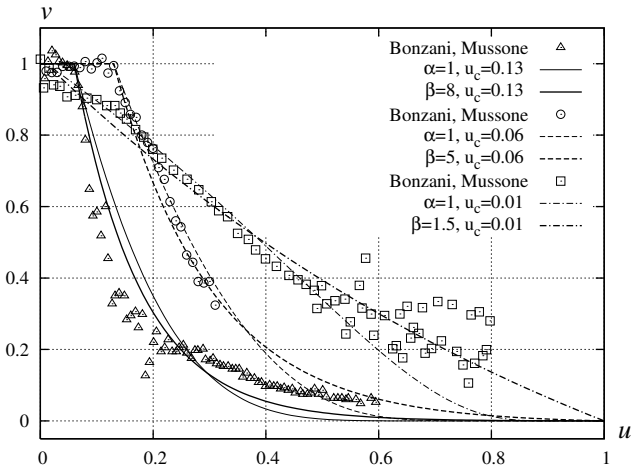

Figure 1: Fitting to experimental data on vehicular traffic [24] for different values of α and β

where $Z(t)$ is the generalized non-dimensional coordinate that expresses the motion of the system while the generalized non-dimensional properties are:

$$m^* = \int_0^L m(x,t)\varphi(x)^2 dx, \tag{6}$$

$$k^* = \int_0^L k(x,t)\varphi(x)^2 dx, \tag{7}$$

$$c^* = \int_0^L c(x,t)\varphi(x)^2 dx, \tag{8}$$

$$F^*(t) = \int_0^L F(x,t)\varphi(x) dx, \tag{9}$$

where m is the total mass (structural and added mass) and $c(m,k)$ is the viscous proportional structural damping [22].

2.3 Crowd-structure interaction

The crowd system and structural system display a two-way interaction. In order to model its complexity, the following assumptions seem to be reasonable:

- the motion of the platform, described by its velocity, reduces the walking velocity;
- the pedestrians adjust their step to the platform motion with a synchronization time delay $\Delta\tau$. Generally speaking, the time delay is expected to be greater than the time interval between two succeeding footfalls;
- after the pedestrians have stopped because of excessive lateral vibrations at time t_s, a stop-and-go time interval Δt_r should elapse before they start walking again.

The structure-to-crowd interaction is made possible through a suitable adaptation of closure equation 4. The crowd velocity v, previously expressed only as a function of the density u, is multiplied by a corrective factor h that makes v sensitive to the platform velocity. In order to define h, let us introduce the pointwise local maxima ζ_p of the deck velocity $\dot{z}$ defined as:

$$\zeta_p = max(|\dot{z}|). \tag{10}$$

The continuous function $\zeta(t,x)$ is obtained by interpolating the local maxima ζ_p and represents the envelope of the platform velocity time history in each of its points (Fig. 2).

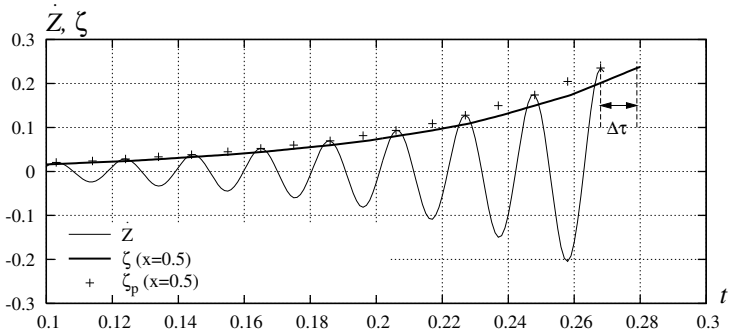

Figure 2: Time history of the generalized force $\dot{Z}$ and envelope of the local maxima ζ

The corrective factor $h(t,x)$ is defined as:

$$h(t,x) = \begin{cases} 1 - \frac{\zeta(t-\Delta\tau,x)}{\bar{\dot{z}}} & \zeta \leq \bar{\dot{z}} \cap t \geq t_s + \Delta t_r \\ 0 & \zeta > \bar{\dot{z}} \cap t_s < t < t_s + \Delta t_r \end{cases} \tag{11}$$

where $\bar{\dot{z}}$ is a stop-threshold value obtained from a limit on the deck displacement amplitude proposed in [26]; it represents the level of lateral vibration above which pedestrians feel unsafe and stop walking. It is worthwhile to point out that $h(t,x)$ is defined in the domain [0;1]. The complete expression of the closure equation is graphically represented in Fig.3.

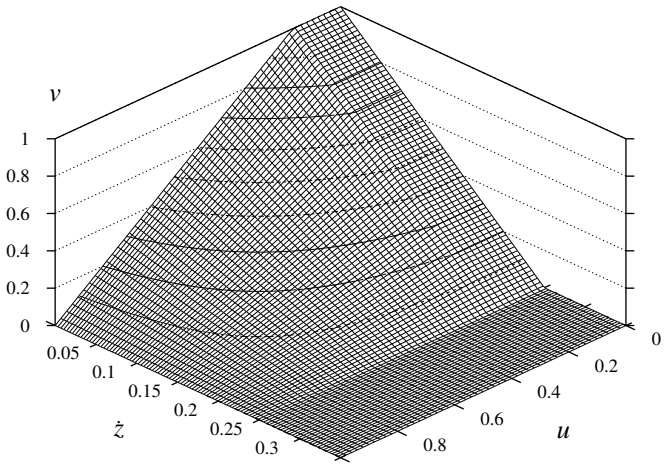

Figure 3: Closure equation $v = v[u, \dot{z}]$

The crowd-to-structure interaction takes place in two ways. On one hand, the structural mass $m_s(x)$ is constantly updated, including the crowd added mass $m_c(x,t)$. On the other hand, the total lateral force F exerted by pedestrians is expressed as:

$$F(x,t) = fuS, \tag{12}$$

where f is the lateral force of a single pedestrian and S is the synchronization coefficient.

The force is assumed to be linearly dependent on the platform velocity, as results from a fitting to experimental data [3]. In Fig.4-a, the force $f(\dot{z})$ is represented in terms of DLF. Furthermore, the force of one pedestrian depends on the walking velocity, as stressed by Wheeler [5], as far as the force vertical component is concerned. Because of the lack of information concerning the relationship between the lateral force and the walking velocity, a law is herein proposed to take into account the reduction of the force amplitude when walking the velocity decreases:

$$g(v) = 1 - \exp(-\gamma v), \tag{13}$$

where γ is a parameter that has to be experimentally obtained, whose trial value is set equal to 20 in the following. The complete expression of $f(\dot{z}, v) = f(\dot{z}) \cdot g(v)$ is represented in Fig.4-b in terms of DLF.

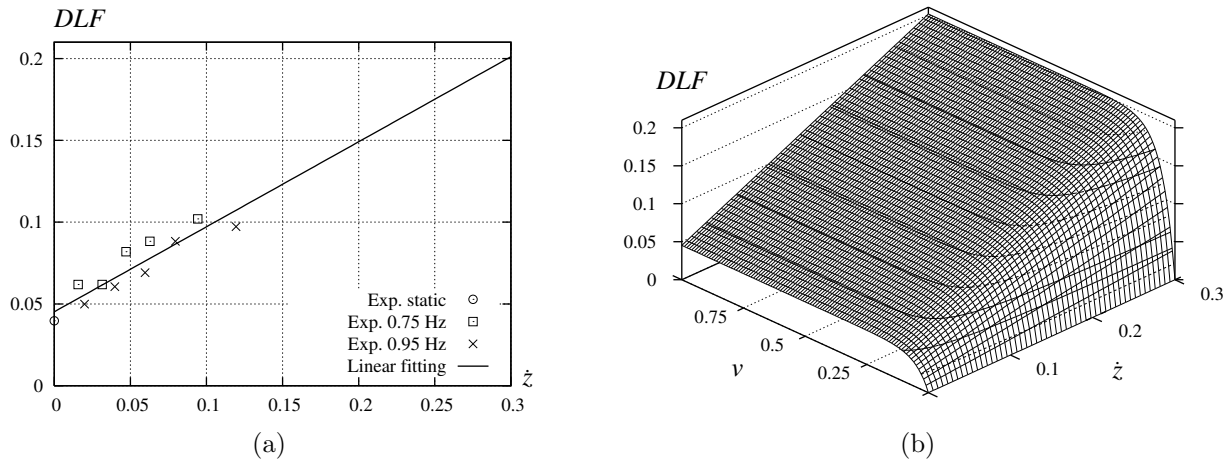

(a) (b)

Figure 4: Single pedestrian lateral force

The synchronization coefficient S is expressed as the sum of two terms in order to take into account both the synchronization between one pedestrian and the structure and synchronization between pedestrians:

$$S(\zeta, u) = S_{ps}(\zeta) + S_{pp}(u). \tag{14}$$

The first term, $S_{ps}(\zeta)$, is defined as a piecewise function (Fig.5-a): the first branch follows from a quadratic fitting to experimental data from laboratory tests [3]; the second branch shows a qualitative distribution based on the consideration that, as ζ approaches the stop-threshold value, the pedestrian is supposed to loose his synchronization. The second term, $S_{pp}(u)$, is defined in a qualitative way because of the scarceness of experimental data. S_{pp} develops upon the following assumptions: for values of u lower than u_c, no synchronization between pedestrians takes place; for intermediate values of u, a little variation in the density causes a great increase in S_{pp}, while the synchronization between pedestrians increases more slowly as the value of u approaches its bounds (Fig.5-b).

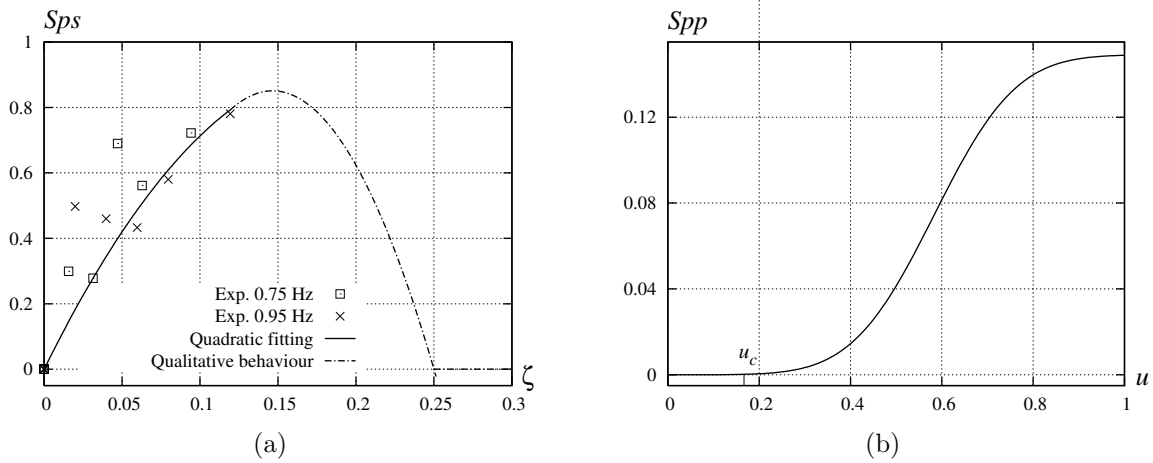

(a) (b)

Figure 5: Synchronization coefficients

It is worthwhile to point out that most of the laws presented in this section come from qualitative considerations about pedestrian behaviour and are rarely supported by experimental data, due to their scarceness in literature. Neverthless, a specific test can be conceived for each of the introduced parameters, so that their identification is foreseeable.

3 Computational approach

The solution of the mathematical model is obtained by means of computational simulation performed in the space and time domains. The partitioned analysis of the coupled system allows the two-solver approach [20] sketched in Fig. 6 to be used. It follows that each field can be treated with discretization techniques and solution algorithms that are known to perform well for the isolated system.

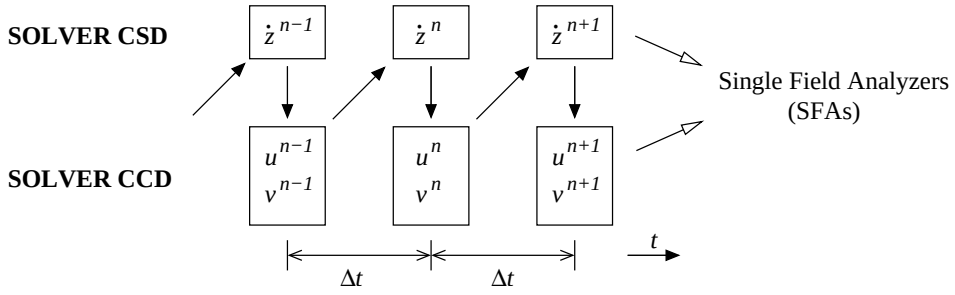

Figure 6: Flowchart of the two-solver approach

The Computational Crowd Dynamics (CCD) solver employes the Finite Difference Method to obtain the approximate solution to the Partial Differential Equation (PDE) governing the crowd dynamics. Four different numerical schemes have been tested to work out the appropriate one. The schemes are implemented in their conservation form to guarantee that we converge to the solution [27]. The Upwind (UP) and Lax-Friederichs (LF) schemes are first order ones; the other two schemes, i.e. the Lax-Wendroff (LW) and MacCormack (MC) ones, use a two-step splitting technique to achieve second order accuracy. The Computational Structure Dynamics (CSD) solver employes a 4th order Runge-Kutta scheme to solve the Ordinary Differential Equation (ODE) that describes the SDOF structural subsystem.

Some *a-priori* considerations about the computational grids can be drawn. The crowd and structural dynamics have quite different space and time scales. As far as the space discretization step Δx is concerned, the traffic phenomena in fact require a dense computational grid because of the possibility of the occurence of high density gradients. On the other hand, the frequency of the first lateral mode usually falls in the lock-in region for the structures of interest: hence, a coarser grid can be used to describe the corresponding mode shape. In order to take into account this difference, the space domain is first partitioned field-by-field, and then each field is separately discretized. The resulting so-called differential partitioning permits non matching meshes to be generated in the crowd field (subscript c) and structural field (subscript s) and a relevant reduction of the computational costs of the modal analysis to be obtained. Data interpolation between non matching grids is obtained by means of quadratic interpolation of the eigenvector φ_s. Furthermore, the non dimensional step Δx_c should satisfy the continuity assumption of the model. It follows that it has a lower bound equal to the space occupied by one pedestrian in a condition of congested traffic, i.e. $\underline{\Delta x}_c = 1/(u_M \cdot BL)$. A similar problem arises for the time discretization step Δt. The characteristic time of the structure, that is, the period of oscillation of interest $0.83 \leq T_s \leq 1.25$ sec, is much smaller than the crowd characteristic time T_c, defined in Section 2.1. It follows that the structural field requires a finer time grid in order to fully describe the dynamics of the structure. Bearing this in mind, a common non dimensional time step $\Delta t \approx T_s/20T_c$ is recommended for the proper simulation of both phenomena.

The two way interaction between the two subsystems is summarized in the flowchart of Fig. 7. It is worth stressing that the described solver couples different mathematical tools related to different models and problems. Each specific tool can possibly be improved in view of a conceivable development in various fields, e.g. controllability problems and/or modelling thermal effects [28]. Dealing with complex geometries may need adaptative finite difference solvers [29]. On the other hand, each technical development should be related to the above multiscale solver.

4 Applications and results

The proposed model is applied to a benchmark footbridge characterized by the following parameters:

$L = 90$ m;

$B = 4$ m;

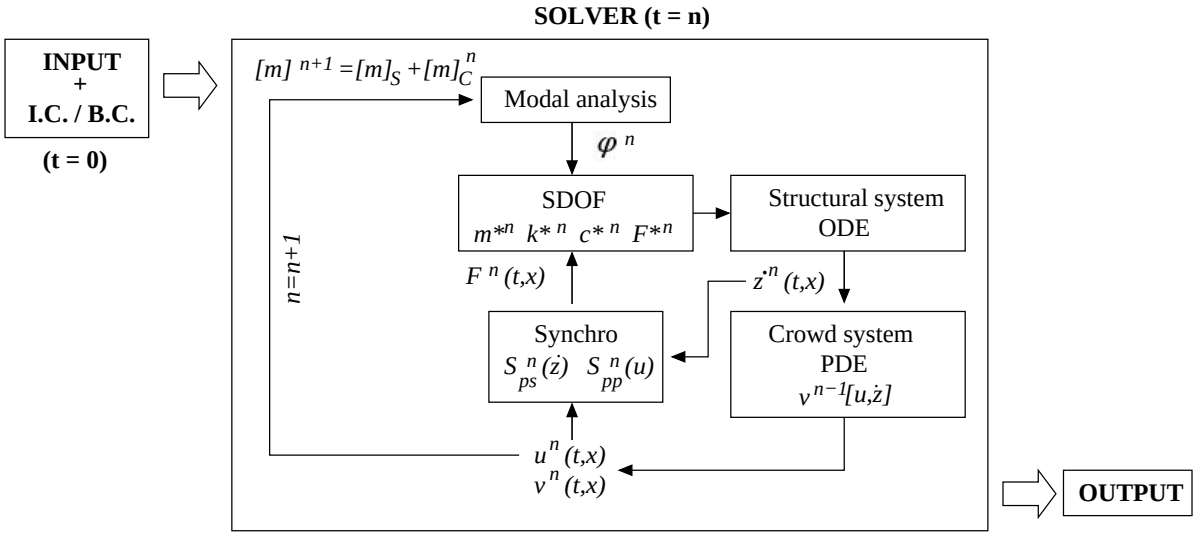

Figure 7: Flowchart of the crowd-structure interaction

$m_s = 500$ kg/m^2;
$\xi = 0.005$;
$\omega = 2\pi \cdot 0.9$ rad/sec,
where m_s is the structural mass, ξ is the damping ratio and ω is the initial damped circular frequency.

4.1 Computational optimisation

Since the model deals with a complex non linear coupled system, an *a-priori* choice of the most appropriate numerical scheme and computational grid is not possible. Hence, the optimization of the computational parameters is performed first on a model equation, then for the crowd system only and finally for the crowd-structure interaction.

4.1.1 Crowd system: Burgers' model equation

In order to choose the most suitable numerical scheme and grids to solve the PDE, the four previously cited schemes are tested on a non linear hyperbolic model equation (Burgers' equation, $v = u$) with Heaviside initial conditions (i.c.)

$$u(x,0) = \begin{cases} u_l & x < 0.2 \\ u_r & x > 0.2 \end{cases} \tag{15}$$

for which the analytical solution is available (Riemann problem) [27] in two cases: $u_l > u_r$ (shock wave) and $u_l > u_r$ (rarefaction wave). Fig. 8 shows a comparison between the exact and approximate solutions at t=0.5, obtained with the different numerical schemes and same discretization in time and space (Δt=1/1000, Δx=1/320).
As expected, the first-order schemes show the well-recognized diffusive effect while the second-order schemes show unphysical oscillations, especially upstream to the discontinuity. Both effects are due to the truncation error of the schemes, which is proportional to a power of the space discretization step Δx_c.

A parametric study on space discretization is then performed for each numerical scheme in the case of shock waves. The space step is systematically refined in the range [$\underline{\Delta x_c}$=1/640;1/40], with a ratio of two between two successive grid sizes. The accuracy of each scheme is evaluated by means of three parameters measured in x=0.4 and t=0.5: i. the phase error between the approximate and exact solution expressed as $\epsilon_{ph} = (u_{approx} - u_{exact})/(u_l - u_r)$; ii. the diffusion evaluated by $\epsilon_d = (\partial u/\partial x)^{-1}$; iii. the maximum oscillation of the solution, which is typical of second order schemes, calculated as $\epsilon_o = (u_{max} - u_l)/(u_l - u_r)$ (Fig. 9).
An error threshold of 5% is fixed in order to determine the optimal space step Δx_c for each method. Fig. 9-c shows that LF and MC schemes do not satisfy the imposed limit on oscillations, therefore they are not suitable for the applications discussed in this paper. It is worth pointing out that the Burgers' equation always involves the forward propagation of the initial discontinuity, therefore it is not suitable to model all

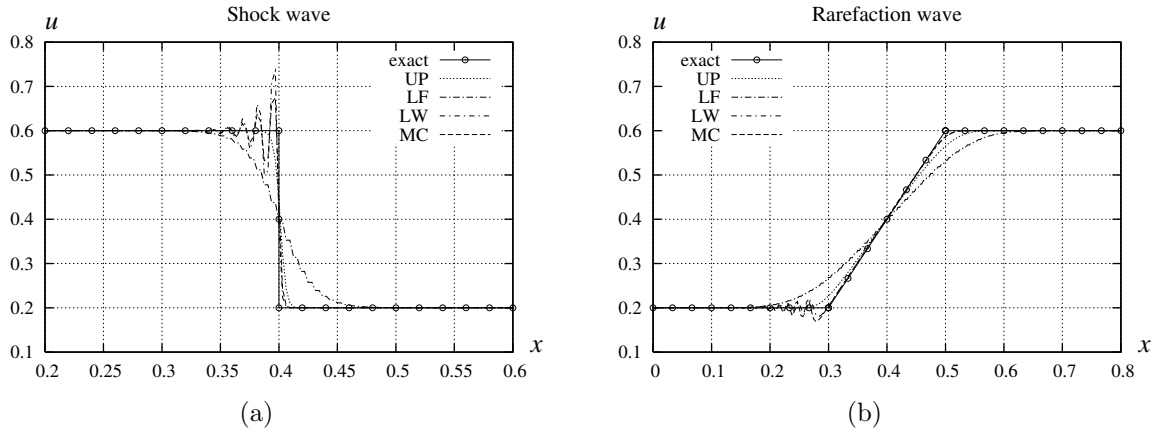

Figure 8: Comparison between the exact and approximate solutions of the Riemann problem

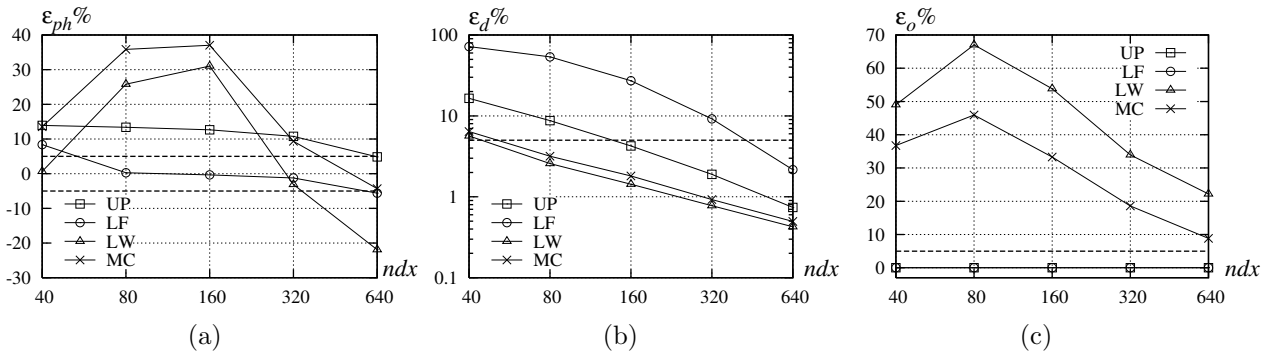

Figure 9: Evaluation of the accuracy of the numerical schemes ($t = 0.5, x = 0.4$)

the different flow regimes. Hence, in the following section the UP and LF schemes are tested on the adopted closure equation (eq. 4) in a case of a backward moving flow.

4.1.2 Crowd system: actual closure equation

In the following, the closure equation 4 is adopted with $\beta = 0$ and i.c. on u expressed through the error function (erf):

$$u(x,0) = u_r + \frac{\Delta u}{2}\left\{1 - erf\left[\frac{0.2}{L}(x - 0.5L)\right]\right\}, \tag{16}$$

where $\Delta u = u_l - u_r$. The values of u_l and u_r are chosen in order to have a negative solution propagation speed (backward moving flow), specifically $u_l = 0.8$ and $u_r = 0.7$. Fig. 10 shows the results of the parametric study on space discretization. Since the exact solution is not available, the errors are evaluated with respect to an approximation of the exact solution calculated for $\Delta x_c = 1/1280$ by means of the Richardson extrapolation [30].
As expected, the overall order of the schemes is also confirmed using the actual closure equation. In particular, the UP scheme satisfies the afore mentioned threshold value for diffusion with $\Delta x_c \leq 1/320$.

The definitive choice of the numerical scheme and space step Δx_c will be assessed after a crowd-structure simulation is performed in the following section.

4.1.3 Crowd-Structure Interaction

A parametric study on Δx_c is finally performed for both numerical schemes in the case of a crowd-structure interaction simulation with a constant initial distribution of the crowd density $u(x,0) = 0.6$ and null initial displacements and velocity of the platform. The effects of the schemes and grid spacing are evaluated considering the spatial distribution of the crowd density at $t = 1.5$ (Fig. 11-a) and the time history of the platform velocity at midspan ζ (Fig. 11-b).

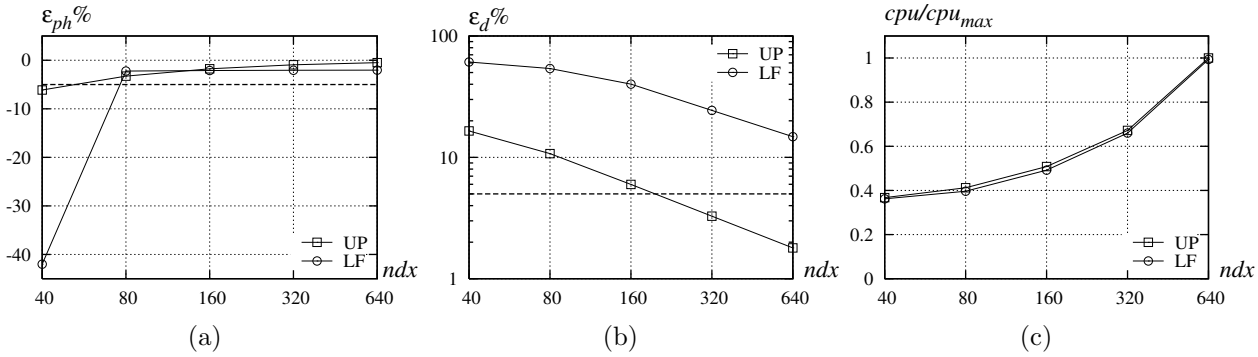

Figure 10: Evaluation of the accuracy of the UP and LF schemes ($t = 0.3, u = 0.75$)

The higher diffusive effect introduced by the LF scheme is confirmed once more. Neverthless, new effects on the crowd dynamics are introduced by the platform velocity when it exceeds its stop-threshold value $\bar{\bar{z}}$ (eq. 11). In particular, discontinuities in the crowd velocity and density arise (Fig. 11-a). The duration in time of these discontinuities is due to the hyperbolic nature of the adopted governing equation, while the pedestrians actually tend to smooth density gradients. Moreover, high gradients can induce numerical instability. Both the above mentioned problems can be avoided by introducing numerical diffusion. Conversely, excessive diffusion can hide some interesting local phenomena, like the ones that occur when the stop-and-go time interval has elapsed and pedestrians restart walking. The time history of the platform velocity at midspan ζ (Fig. 11-b) clearly shows the convergence of the solution of the crowd-structure system for higher refined grids. Bearing these considerations in mind, the UP scheme with $\Delta x_c = 1/640$ is retained.

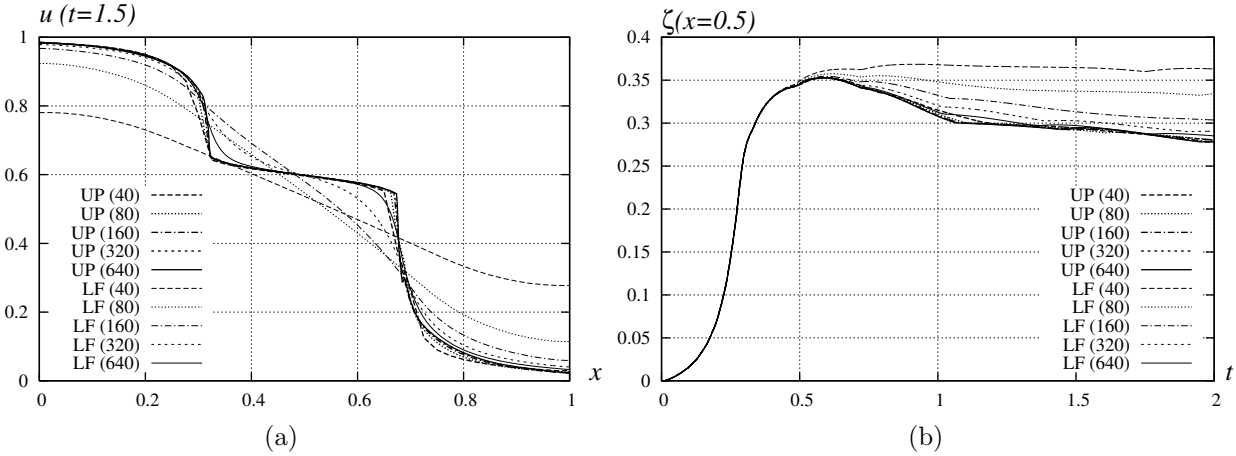

Figure 11: Parametric study on Δx_c: crowd density at $t = 1.5$ (a) and platform velocity at midspan (b)

4.2 Parametric study on flow regimes

The sensitivity of the solution to different initial crowd densities is evaluated in order to assess the capability of the model to predict free and congested flow regimes. The i.c. on u are expressed through equation 16.

First, a parametric study is performed varying the values of u_r in the range [0; 0.9], with $\Delta u = 0.1$. The results of the simulations at $t = 0.4$ are scaled with respect to Δu in Fig. 12-a and three meaningful cases are plotted in Fig. 12-b. The figure points out that the increase in the initial value of u_r causes a decrease in the solution propagation speed. It follows that there is a value of the initial density that marks the transition between a free and a congested regime. It is worth stressing that the discontinuity of the solution when $u_r = 0.1$ is due to the discontinuity in the adopted closure equation for $u = u_c$, as shown in Fig. 12-b.

Hence, a parametric study on Δu is performed, first by taking a constant value of $u_r = 0.1$ (Fig. 13), then by considering a constant value of $u_l = 0.9$ (Fig. 14). It could be observed that an increase in the value of Δu causes a further smoothing of the initial perturbation on u. This result could be commented on, from a phenomenological point of view, by stating that, the higher the difference between the density in the inlet and in the outlet, the higher the homogeneization of the density space distribution as time elapses.

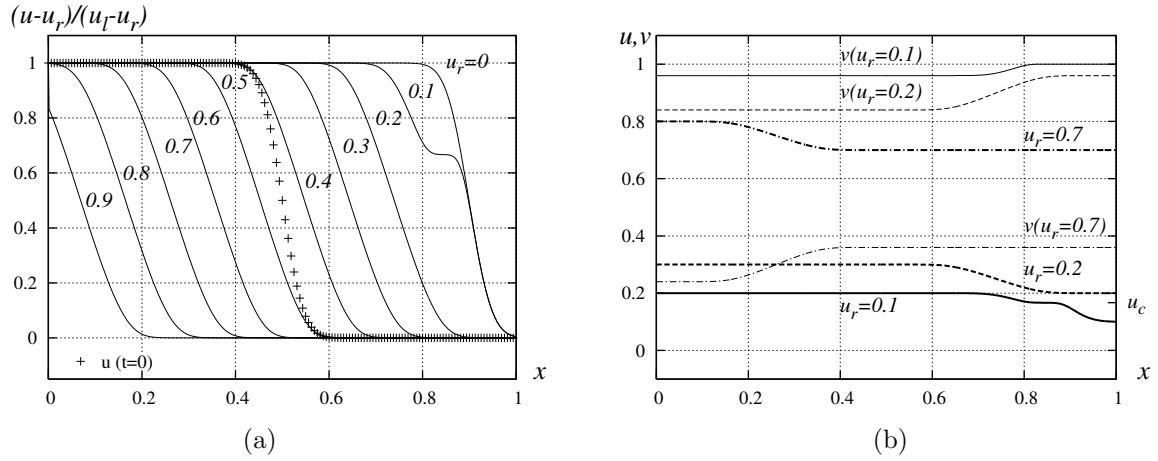

(a) (b)

Figure 12: Parametric study on u_r with the UP scheme ($t = 0.4$)

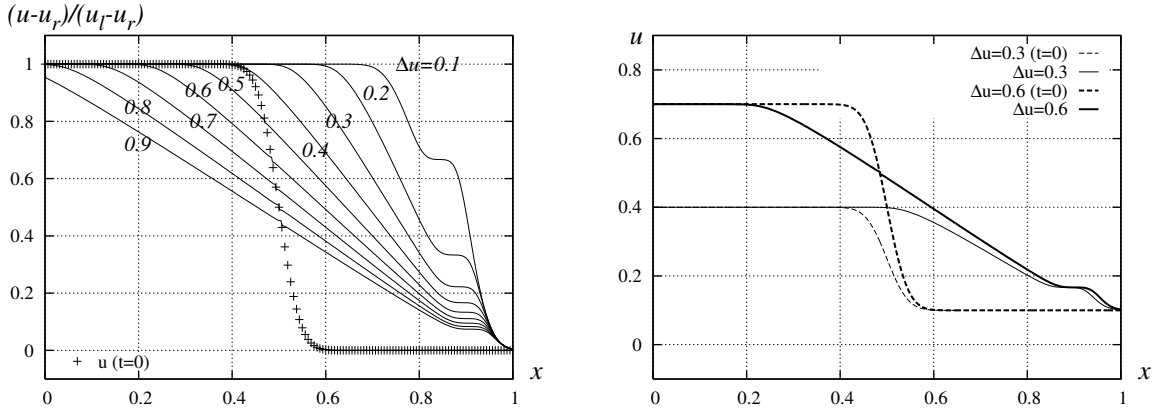

(a) (b)

Figure 13: Parametric study on Δu with constant u_r ($t = 0.4$)

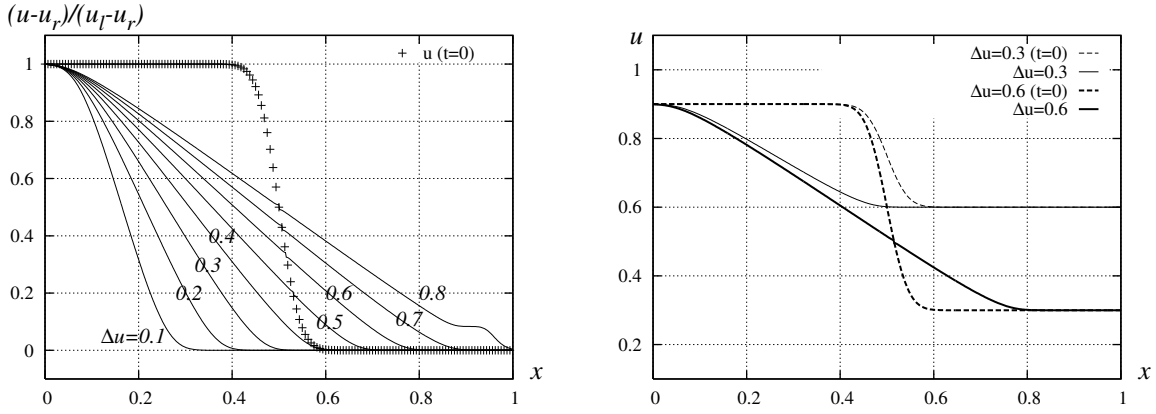

(a) (b)

Figure 14: Parametric study on Δu with constant u_l ($t = 0.4$)

4.3 Parametric study on runnability conditions

A parametric study on the influence of the parameter β is performed, in order to evaluate the sensitivity of the crowd flow to the runnability conditions of the motionless platform.

Two kinds of simulations are carried on. The first ones are based on an erf distribution of $u(x, 0)$ ($u_l = 0.3$, $\Delta u = 0.1$) and a constant distribution of β along the deck, with β ranging from 0 to 10, in order to simulate

different homogeneous degrees of runnability. Fig. 15-a shows the evolution in time and space of u for $\beta = 6$: the initial perturbation moves backwards without growing in amplitude. Fig. 15-b shows istantaneous distributions of u at $t = 0.4$. It indicates that there is a critical value of β that marks the transition between a forward and a backward moving front. It is worth pointing out that the critical value of β is expected to change for different values and distribution of the initial density.

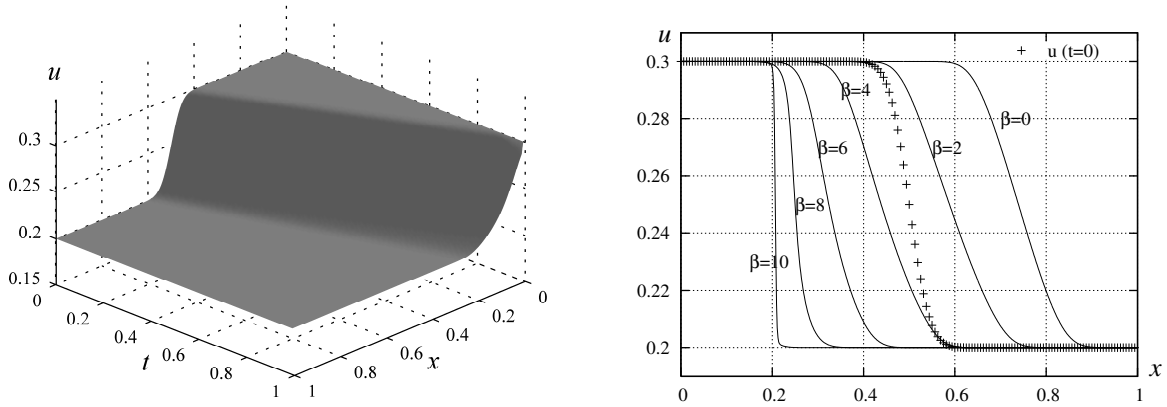

(a) (b)

Figure 15: Parametric study on β

In the second kind of simulations, $u(t = 0) = 0.2$ is kept constant along the deck and β varies in space with a normal distribution centered in the midspan, in order to take into account non homogeneous environmental conditions such as a panoramic point in the middle of the span. Fig. 16-a shows the evolution in time and space of u for $\Delta\beta = 6$: the density locally increases upstream to the midspan, while it decreases downstream. The local congested traffic moves backwards, but the fully congested regime is never reached. Fig. 16-b summarizes the istantaneous distributions of u obtained for the different values of $\Delta\beta$ at $t = 0.4$. The higher the discontinuity in the runnability conditions, the more relevant the perturbation and the faster its backward propagation.

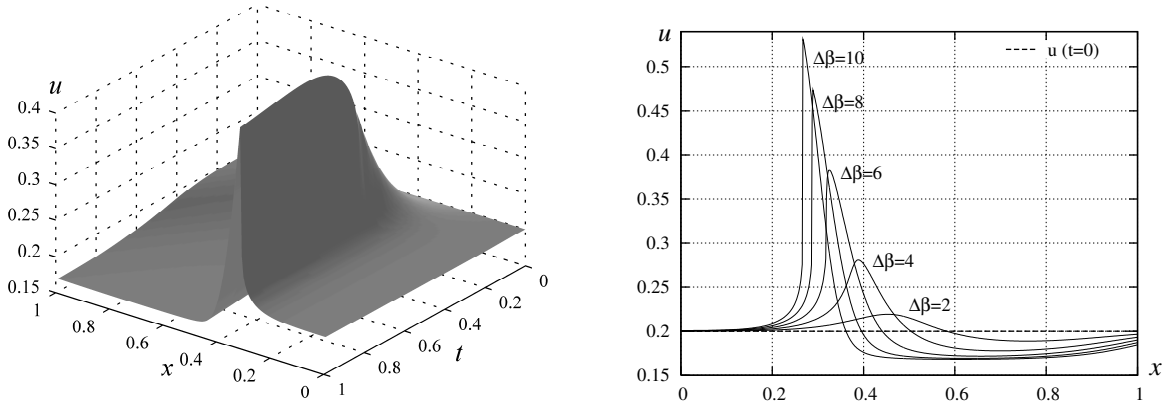

(a) (b)

Figure 16: Parametric study on $\Delta\beta$

4.4 Simulation of the crowd-structure interaction

The last part of the work is devoted to the application of the model in the case of crowd-structure interaction. Both parameter β and the crowd density have an initial constant distribution along the span: in such a condition, if the platform is motionless, the crowd flow remains constant in space and time. In particular, $\beta(x, t) = 0$ and a value of $u(x, 0) = 0.6$ is chosen so that the density is high enough to quickly induce synchronization phenomena. In order to better evaluate the fully-developed interaction phenomena, the

simulated time is twelve times the characteristic time T_c.

The main variables concerning the crowd system, u and v, are plotted in Fig. 17. A region of motionless pedestrians is clearly visible around the midspan. This phenomenon is expected to be due to the motion of the platform, since the density value is lower than unit. Because of the strict correlation between the crowd and the structural variables, the results can be better commented on looking at the graphs in Fig. 18, which contain both the time history of the generalized properties and some significant instantaneous spatial distributions of u and v. It is worth stressing that the structural variables are expressed in dimensional form in order to permit an engineering and physical evaluation of the results to be made.

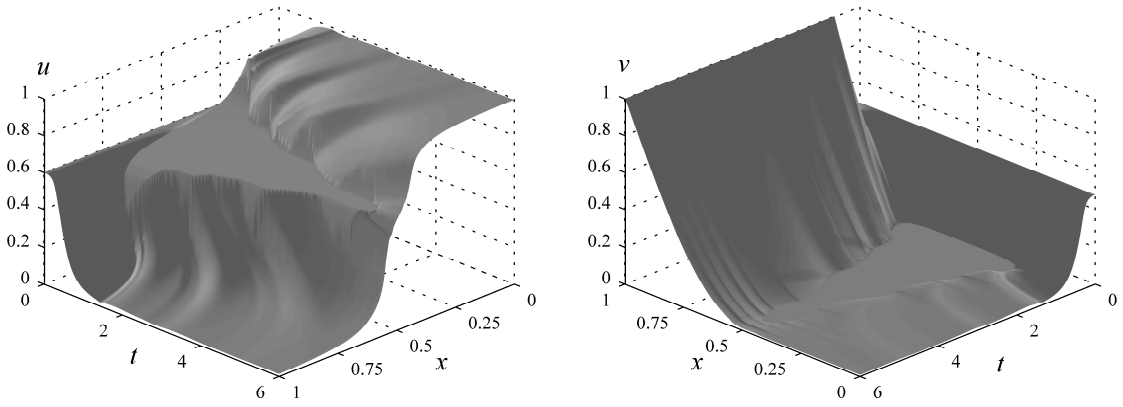

(a) (b)

Figure 17: Crowd density u (a) and pedestrian velocity v (b) versus x, t

The following considerations can be drawn:

- at $t = 0.1$, the force starts to grow because of the deck motion, since the density is still constant along the span. v has a distribution that traces the modal shape of the deck;
- at $t = 0.28$, the platform velocity exceeds the stop-threshold value at midspan, causing the pedestrians to stop walking. As a consequence, the generalized force starts decreasing and the density grows in the first half of the span, i.e. upstream to the motionless people;
- at $t = 0.57$, $\dot{Z}$ reaches its maximum amplitude. The stop-threshold value has been surmounted in a large tract of the span: a greater number of motionless pedestrians causes the total force to decay and a traffic jam to arise upstream, while the density decreases downstream since the crowd can walk faster;
- at $t = 2$, $\dot{Z}$ is decreasing because of the smaller force exerted on the structure. It follows that a certain number of pedestrians who were still restart walking: the congested front moves forwards in the first half span, while in the second half the density decreases even more;
- at $t = 5.45$, $\dot{Z}$ is below the stop-threshold value throughout the span. The people in the first half span are motionless because of the crowd density, which is near unity, while, once the midspan is passed, v grows quickly and the deck is almost empty;
- the time history of the structural response (Fig. 18-b) shows that, after a transient regime, a steady-state condition is reached. It is characterized by a self-limited amplitude in analogy with the lock-in phenomenon that occurs in wind-structure interaction;
- finally, in order to foresee long term crowd dynamics, let us look at the istantaneous distributions of u and v at $t = 12$: these are similar to the last ones that were described, but the people at the midspan are no longer motionless and the congested front is therefore moving backwards, which means the deck is slowly vacating.

Interesting considerations can be drawn from an observation of both graphs in Fig. 17 and the one in Fig. 19-a, which represents the flux $q = u \cdot v$. A non monotonic reduction of the length characterized by null flux can be observed. At the upstream and downstream limits of the above mentioned length, some perturbations

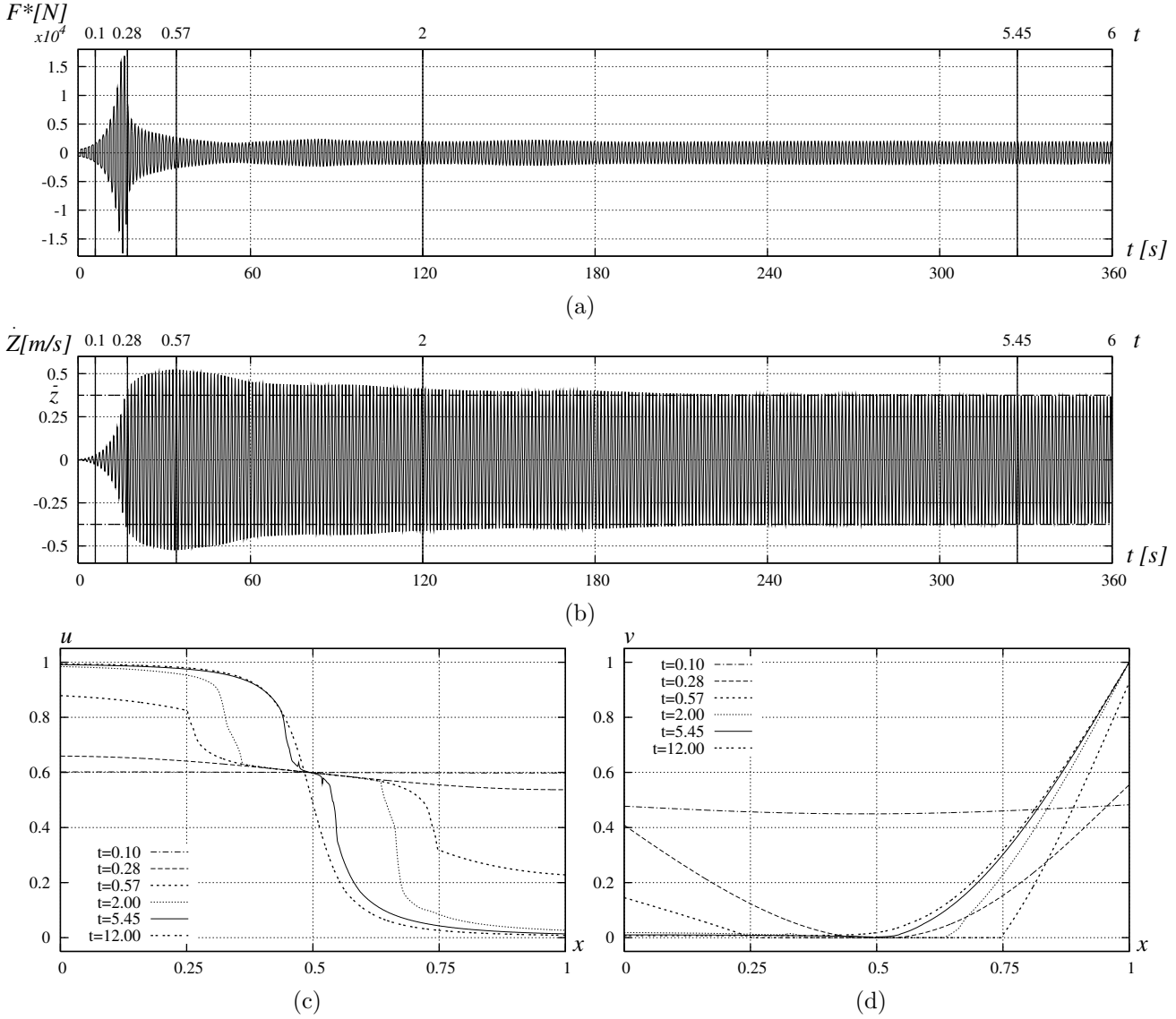

Figure 18: Time history of the generalized force (a) and platform velocity (b), istantaneous spatial distributions of u (c) and v (d)

arise locally and propagate. The phenomenon can be better analyzed focussing on the istantaneous spatial distributions of q for $t = 0.3 \div 0.46$ and $x > 0.5$ (Fig. 19-b). At time $t = 3$, the platform velocity exceeds the stop-threshold value at $x \approx 0.61$. Because of the structural damping and of the force reduction, the platform velocity decreases and the non-null flux moves backwards towards the midspan until $x \approx 0.53$ at $t = 4.2$. This means that a platoon of pedestrians restarts walking, causing the force to grow again (stop-and-go traffic). At $t = 4.4$, the non-null flux in fact starts moving forwards because the platform velocity increases and the stop-threshold value is surmounted once more at $x \approx 0.54$.

The relationships between the total lateral force F and its components, i.e. the single pedestrian force f and the synchronization coefficients S_{ps} and S_{pp}, are summarized in Fig. 20. The forces are expresses in their dimesional form: the single pedestrian force (Fig. 20-c) is intended as the theoretic force exerted by one fully synchronized pedestrian at position x and time t; the total force F is the force per unit length exerted by the actual number of synchronized pedestrians. The following observations can be made:

- the synchronization coefficient S_{pp} has the same evolution as u, since it is only a function of the density;
- since the deck is initially motionless, S_{ps} is null at $t = 0$. Hence, the overall synchronization is only a function of the crowd density, i.e. the lateral force exerted by pedestrians depends on S_{pp};
- the synchronization coefficient S_{ps} reaches its maximum value for values of ζ near to 0.15 (Fig. 5-a),

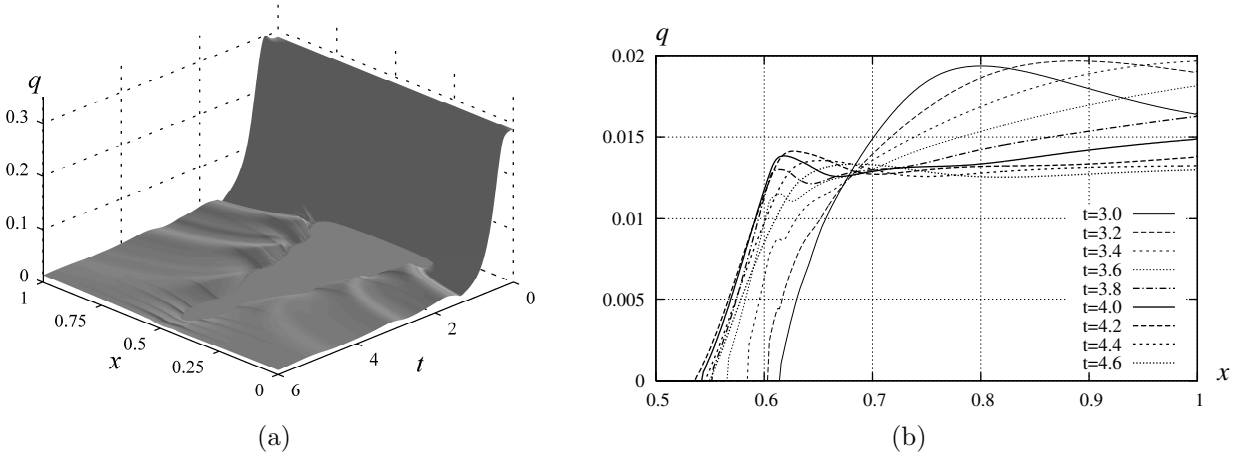

(a) (b)

Figure 19: Crowd flux q versus x and t (a) and istantaneous spatial distributions (b)

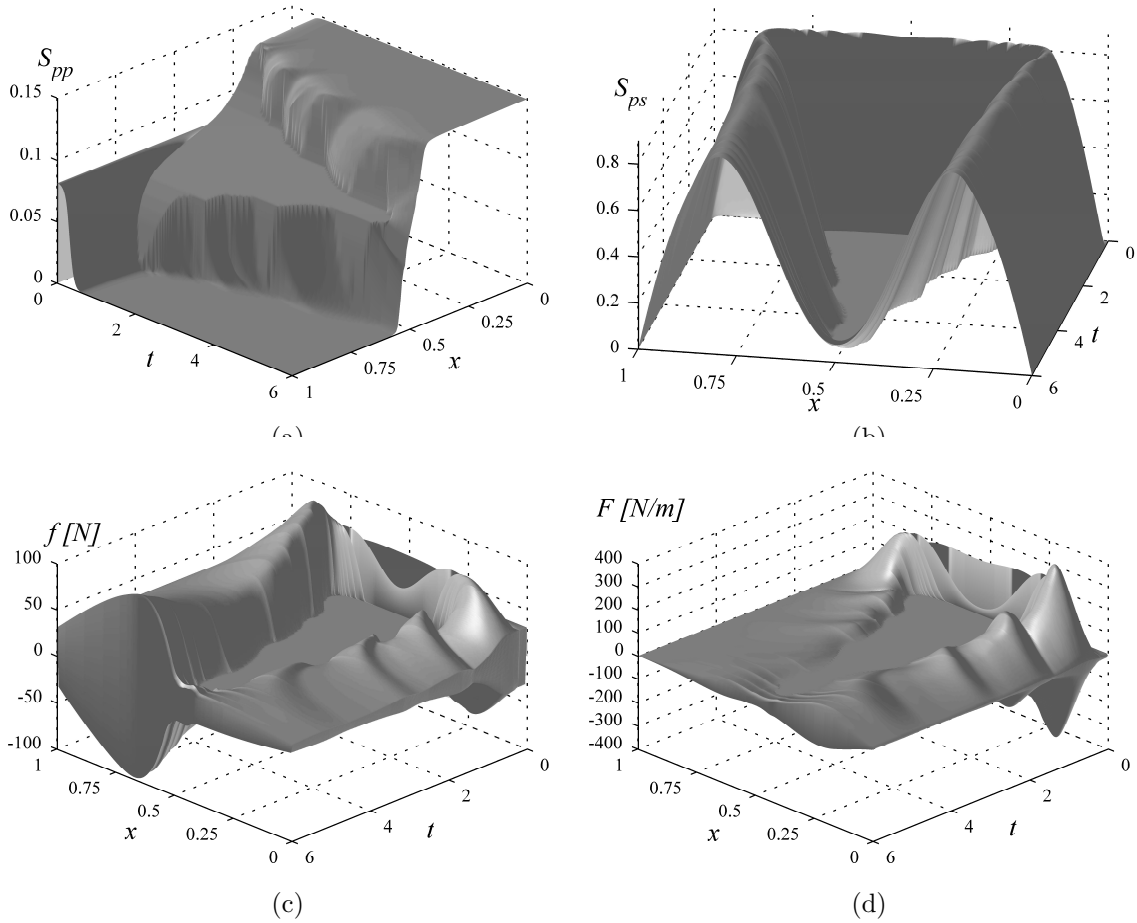

(c) (d)

Figure 20: Synchronization coefficients (a,b), single pedestrian force f (c) and total lateral force F (d) versus x, t

while it falls to zero when ζ reaches the stop-threshold value, since the pedestrians are motionless;

- the single pedestrian force attains high intensities ($f \approx 90$ N) downstream to the midspan stopped traffic because both the platform and the crowd velocity have relevant values. Neverthless, the total actual force shows low values downstream ($F \approx 50$ N/m), because of the reduced number of pedestrians (i.e. reduced crowd density).

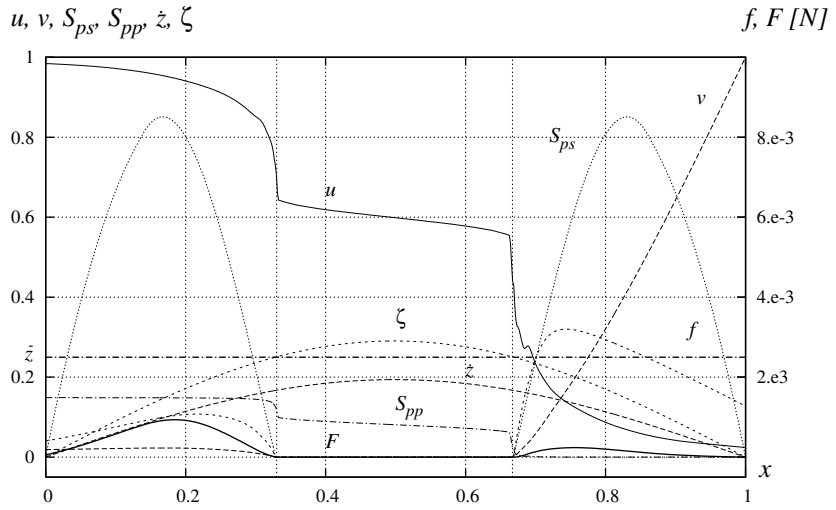

Figure 21: Relationships between the variables involved in the problem ($t = 1.5$)

What has been stated so far is summarized in Fig. 21, which illustrates the correlations among all the non dimensional variables involved in the problem. In particular, it is worth stressing the relationship between the platform velocity ζ and the crowd density and velocity once more: in the region of the deck where ζ exceeds the stop-threshold value, v is null and u has a discontinuity at the boundary of the previously mentioned region.

5 Concluding remarks and research perspectives

The present paper discusses the possibility of modelling the complex multi-physical non-linear coupled system that results from a crowd-structure interaction using the computational approach. The presented mathematical model permits several non-linear features of the problem to be taken into account, that is, effects of discontinuities in the crowd flow such as obstructions, traffic jams, stop-and-go phenomena. Thanks to the post processing facilities of the computational tool, the proposed approach allows the physical interpretation of the interaction between the structure and the pedestrians to be attained. Hence, the proposed model contributes to give a deeper insight into the large scale phenomena, that occur in crowd-structure interaction, so far not completely understood. Because of the lack of experimental data, the presented model mainly gives a satisfying representation of the crowd dynamics from a qualitative point of view: further research should be addressed to the determination of the values of the parameters involved by means of *ad hoc* experimental tests. Furthermore, microscopic or mesoscopic models of the pedestrian flow could be included in the framework of crowd-structure interaction.

References

[1] S. Živanovic, A. Pavic, and P. Reynolds. Vibration serviceability of footbridges under human-induced excitation: a literature review. *J. of Sound and Vibration*, 279:1–74, 2005.

[2] Y. Fujino, B. M. Pacheco, S. Nakamura, and P. Warnitchai. Synchronization of human walking observed during lateral vibration of a congested pedestrian bridge. *Earthquake Engineering and Structural Dynamics*, 22:741–758, 1993.

[3] P. Dallard, T. Fitzpatrick, A. Flint, S. Le Bourva, A. Low, R. M. Ridsdill, and M. Willford. The London Millennium Footbridge. *The Structural Engineer*, 79(22):17–33, 2001.

[4] T. P. Andriacchi, J. A. Ogle, and J. O. Galante. Walking speed as a basis for normal and abnormal gait measurements. *Journal of Biomechanics*, 10:261–268, 1997.

[5] J. E. Wheeler. Prediction and control of pedestrian induced vibration in footbridges. *ASCE Journal of the Structural Division*, 108:2045–2065, 1982.

[6] A. D. Pizzimenti and F. Ricciardelli. Experimental evaluation of the dynamic lateral loading of footbridges by walking pedestrians. In *6th International Conference on Structural Dynamics*, Paris, 2005.

[7] A. McRobie, G. Morgenthal, J. Lasenby, and M. Ringe. Section model tests on human-structure lock-in. *Bridge Engineering*, 156(BE2):71–79, 2003.

[8] D. E. Newland. Pedestrian excitation of bridges - recent results. In *10th International Congress on Sound and Vibration*, Stockholm, 2003.

[9] A. D. Pizzimenti and F. Ricciardelli. The synchronization: the lessons of the wind engineering and their application to the crowd-structure interaction. In *8th Italian Conference on Wind Engineering*, Reggio Calabria, 2004.

[10] H. Grundmann, H. Kreuzinger, and M. Schneider. Dynamic calculations of footbridges. *Bauingenieur*, 68:215–225, 1993.

[11] I. Prigogine and R. Herman. *Kinetic Theory of Vehicular Traffic*. Elsevier, New York, 1971.

[12] W. Leutzbach. *Introduction to the Theory of Traffic Flow*. Springer, 1988.

[13] N. Bellomo, M. Delitalia, and V. Coscia. On the mathematical theory of vehicular traffic flow i. fluid dynamic and kinetic modelling. *Math. Models Methods Appl. Sci.*, 12(12):1801–1843, 2002.

[14] D. Helbing, A. Hennecke, V. Shvetsov, and M. Treiber. Micro and macro simulation of freeway traffic. *Mathematical and Computer Modelling*, 35:517–547, 2002.

[15] D. Helbing. Traffic and related self-driven many-particle systems. *Rev. Mod. Phys.*, 73:1067–1141, 2001.

[16] L. F. Henderson. On the fluid mechanics of human crowd motion. *Transportation Research*, 8:509–515, 1974.

[17] S. P. Hoogendoorn and P. H. L. Bovy. A gas-kinetic model for pedestrian flows. *Transportation Research Record*, 1710:28–36, 2000.

[18] D. Helbing. A mathematical model for the behavior of pedestrians. *Behavioral Science*, 36:298–310, 1991.

[19] V. Blue and J. Adler. Emergent fundamental pedestrian flows from cellular automata microsimulation. *Transportation Research Board*, 1644:29–36, 1998.

[20] K. C. Park and C. A. Felippa. Partitioned analysis of coupled systems. In *Computational Methods for Transient Analysis*, chapter 3, pages 157–219. T. Belytschko and T.J.R. Hughes, Amsterdam, 1983.

[21] N. Bellomo and V. Coscia. First order models and closure of mass conservation equations in the mathematical theory of vehicular traffic flow. *CR-Mecanique*, pages 843–851, 2005.

[22] R. Clough and J. Penzien. *Dynamics of structures*. McGraw-Hill, New York, 1987.

[23] H. Bachmann and W. Ammann. Vibration in structures induced by man and machines. In *Structural Engineering Documents*, volume 3a. IABSE, Zurich, 1987.

[24] I. Bonzani and L. Mussone. From experiments to hydrodynamic traffic flow models. I - Modelling and parameter identification. *Mathematical and Computer Modelling*, 37:109–119, 2003.

[25] FIB. *Guidelines for the design of footbridges*, November 2005. Bullettin N.32.

[26] S. Nakamura. Field measurement of lateral vibration on a pedestrian suspension bridge. *The Structural Engineer*, 81(22):22–26, 2003.

[27] R. J. Leveque. *Numerical methods for conservation laws*. Birkhauser, Zurich, 1992.

[28] P. Gervasio and M. G. Naso. Numerical approximation of controllability of trajectories for Euler-Bernoulli thermoelectric plates. *Math. Models Methods Appl. Sci.*, 14:701–733, 2004.

[29] F. Brezzi, K. Lipnikov, and V. Simoncini. A family of mimetic finite difference methods on polygonal and polyhedral meshes. *Math. Models Methods Appl. Sci.*, 15(10):1533–1552, 2005.

[30] J. H. Ferziger and M. Perić. *Computational methods for fluid dynamics*. Springer, Berlin, 2002.